Journal of Nondestructive Evaluation, Vol. 22, No. 4, December 2003 (© 2004)

Residual Magnetic Flux Leakage: A Possible Tool for Studying Pipeline Defects

Vijay Babbar[1] and Lynann Clapham[1,2]

Received May 9, 2002; Revised October 2, 2003

Simulated defects of different shapes and sizes were created in a section of API X70 steel line pipe and were investigated using a residual magnetic flux leakage (MFL) technique. The MFL patterns reflected the actual shape and size of the defects, although there was a slight shift in their position. The defect features were apparent even at high stresses of 220 MPa when the samples were magnetized at those particular stresses. However, unlike the active flux technique, the residual MFL needs a sensitive flux detector to detect the comparatively weaker flux signals.

KEY WORDS: Magnetic flux leakage; residual magnetization; pipeline defects; pipeline inspection; nondestructive testing.

1. INTRODUCTION

The magnetic flux leakage (MFL) technique is frequently used for in-service monitoring of oil and gas steel pipelines, which may develop defects such as corrosion pits as they age in service.(1) Under the effect of typical operating pressures, these defects act as "stress raisers"(2) where the stress concentrations may exceed the yield strength of the pipe wall. The main objective of MFL inspection is thus to determine the exact location, size, and shape of the defects and to use this information to determine the optimum operating pressure and estimate the life of a pipeline. Most MFL tools rely on active magnetization in which the pipe wall is magnetized to near saturation by using a strong permanent magnet, and the flux leaking out around a defect is measured at the surface of the pipeline.[3–5] The magnitude of the leakage flux density depends on the strength of the magnet, the width and depth of the defect, the magnetic properties of the pipeline material, and running conditions such as velocity and stress.(6) A typical peak-to-peak value of leakage flux density from a surface defect may be around 30 G.

Another way of employing the MFL technique for studying the pipeline defects is through residual magnetization. After a magnet is passed over a portion of the steel pipe, some residual magnetization remains. A study of the residual magnetization MFL signal can provide useful information about the size and shape of the defect. However, little published work exists about residual MFL, probably because of the comparatively weak leakage flux signals, which require sensitive detectors. An earlier study of samples magnetized by strong electric currents revealed that the residual flux patterns are basically similar to the active flux patterns, with exceptions that they are very weak and may have opposite magnetic polarity in comparison to the latter.(7) The opposite polarity occurs only when the excitation current is low, whereas for high excitation current level, there is no reversal of polarity. A finite element modeling technique has been proposed by Satish(8) to predict the reversal of the residual leakage field.

The present work investigates the residual flux patterns of defects after the passing of a permanent

[1] Applied Magnetics Group, Department of Physics, Queen's University, Kingston, ON, Canada.
[2] E-mail: lynann@physics.queensu.ca.

0195-9298/02/0600–0117/0 © 2004 Plenum Publishing Corporation

magnet (similar to the situation in pipeline inspection). The residual flux patterns of three different *blind*[3] defects, that is, circular, elongated pit (henceforth named racetrack), and irregular gouge, are investigated. The effect of pipe wall stresses on the active and residual leakage flux signals from some of the defects is also reported.

2. EXPERIMENTAL

Three simulated defects were used in the present study: a circular blind hole, a blind racetrack-shaped defect, and a gouge. The first two defects were produced on the surface of a hydraulic pressure vessel (HPV) constructed for a previous study[9] and were nearly 50% of the wall thickness. These are illustrated in Figure 1. The circular defect has a 15-mm diameter and 5-mm depth; the racetrack has about a 53-mm length, 15-mm width and 4.4-mm depth. An electrochemical-milling process, which prevents the introduction of additional stresses around the defects,[10] was used for creating the first two defects in the HPV. The gouge of about 125-mm length, 26-mm width, and a graded maximum depression of about 14 mm was created on another section of similar steel pipe by using a single backhoe tooth. It is shown in Figure 2.

The HPV used in the present study is shown in Figure 3 and is briefly described here; the details can be found elsewhere.[11] It consists of an outer section of API X70 steel pipeline of 635-mm length, 610-mm diameter, and 9-mm wall thickness separated from an inner steel spool by a hydraulic chamber that contains hydraulic oil. On pressurizing the chamber, circumferential (hoop) stresses can be created in the outer wall of the pipeline and hence the in-service pressure

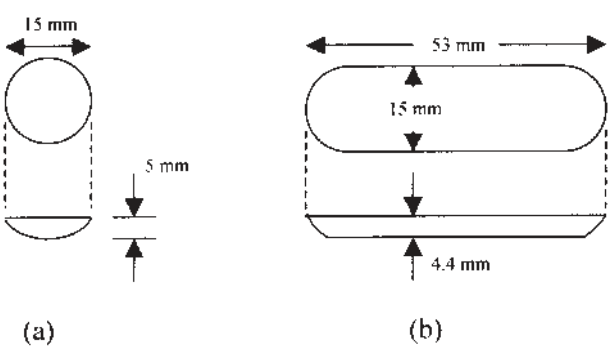

Fig. 1. Geometric details of blind hole (a) and blind racetrack (b) defects.

[3] "Blind" indicates a hole that is not completely through-wall.

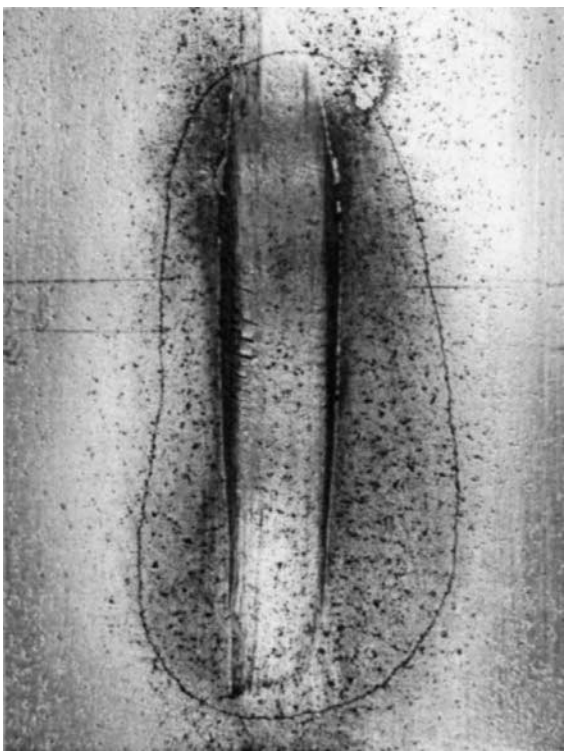

Fig. 2. Camera picture of a gouge on a steel line pipe section. The main groove is nearly rectangular, having dimensions of 53 mm × 15 mm and depth varying from zero to 4.4 mm maximum. An extended depression as indicated by a closed contour is present around the gouge.

stresses can be simulated. Axial stresses are minimized because they are carried by free end caps sealed with O-rings to prevent leakage.

The pipe wall was magnetized by using an assembly of strong permanent magnets. High-strength NdFeB permanent magnet blocks, approximately 55 × 55 × 6 mm^3, were connected in parallel and held in place by aluminum cover plates at each pole piece. Steel brushes, having the same curvature as the pipe, were used to couple the flux into the pipe wall. A back-iron mounting plate was connected to the pole pieces, thus completing the magnetic circuit from the NdFeB magnets through to the pipe wall and back again. To magnetize the defect, the magnet was pulled along the axis and across the surface of the HPV over the defect from left to right with south pole ahead. This is consistent with typical inspection procedures, although in this case the detector is on the outer wall of the pipe while inspection is internal. The magnet was pushed from the pipe end to a cylindrical aluminum platform, where it was lifted off, turned in a direction perpendicular to the axis, and returned to the left of the pressure vessel. This procedure was repeated three times for each magnetization process.

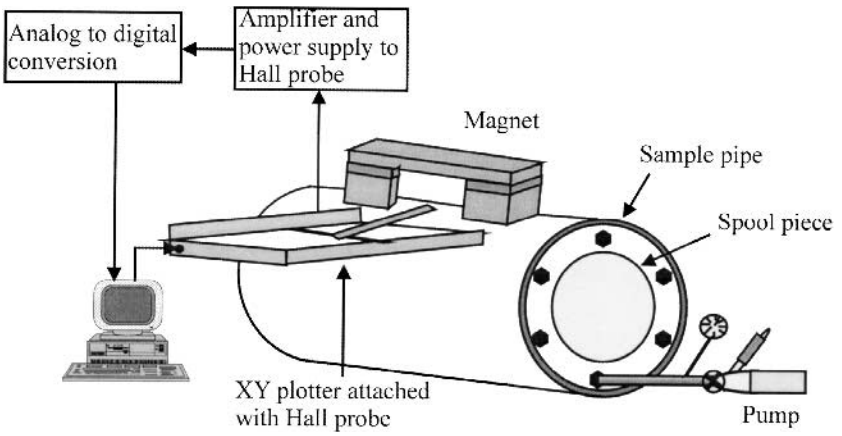

Fig. 3. Outline of pipeline sample (high-pressure vessel), magnet, the Hall probe, and scanning system assembly.

After the three magnetization cycles the magnet remained on the HPV producing a flux density of 1.4 T. The gouge was similarly magnetized. All the measurements were repeated three times with time intervals of several days to verify the reproducibility of results, keeping the direction of magnetization always the same.

The scanning system used in the present investigation can be seen in Figure 3. More details are available in a previous paper.[11] It consisted of an SS94A1 MicroSwitch Hall probe that was controlled by a computer software and moved smoothly over the surface of defects in a two-dimensional grid with increments of 1×1 mm^2. It was connected to a Roland DXY-1100 XY digital plotter, which was controlled by a Tecmar A/D board operated by a compiled Microsoft Visual BASIC 4.0 program called Aquis. Finally, a three-dimensional plotting package called Surfer 7.0 from Golden Software was used for obtaining surface and contour maps.

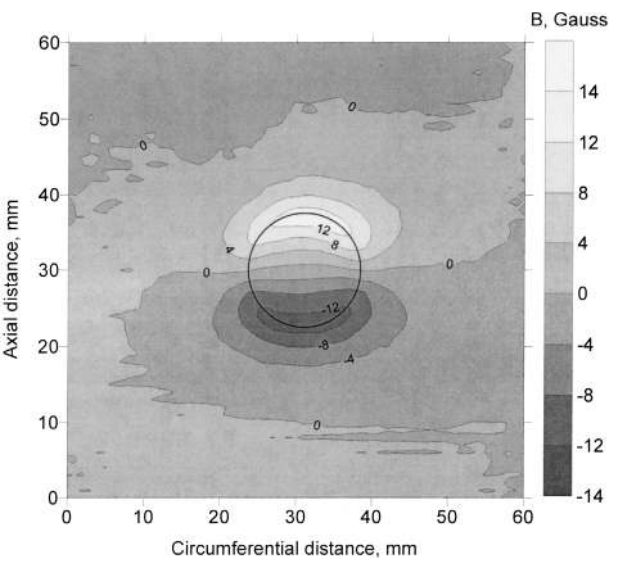

Fig. 4. Contour map of radial active magnetic leakage flux density (B) from circular blind-hole defect. Solid circle represents the actual location of the defect. The applied magnetic field and stress are along the axial and circumferential directions, respectively.

3. RESULTS AND DISCUSSION

3.1 Active and Residual MFL Results in an Unstressed Pipe Wall

The contour map of the active radial MFL scan from the circular blind-hole defect is shown in Figure 4. The magnetic field lies along the axial direction, whereas the stress is circumferential. A corresponding axial line scan through the center of the blind hole is shown in Figure 5, where the solid line is only a guide to the eye. The scan is approximately symmetric along the axis of the pipe; a region of high positive flux is present on one side of the defect and a high negative flux on the other. The peak-to-peak value of the radial leakage flux (MFL_{pp}) is about 27.0 G. The shape of the flux pattern is well understood and has been reported by many workers.[12] Although the size and shape of the circular defect are not obvious from this contour map, some useful information can be obtained. For example, this type of circular defect is typically located between high positive and high negative flux regions, with its center almost on the zero flux line. Also, the MFL_{pp} is used to determine the defect depth. However, for irregular defect shapes, such contour maps may not reveal very useful information about the defect geometry.

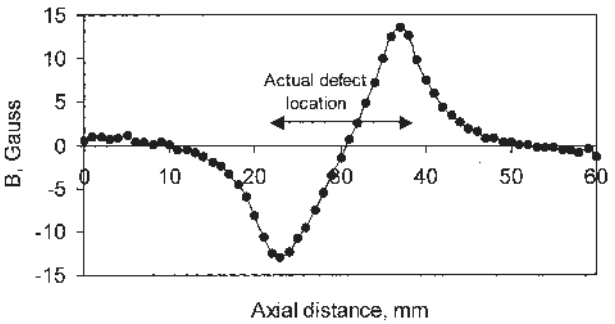

Fig. 5. Radial active MFL axial line scan through the center of the circular defect showing the variation of the radial active magnetic leakage flux density (B) along the axial direction.

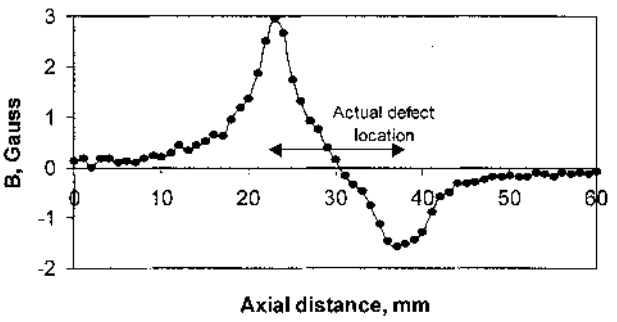

Fig. 7. Radial residual MFL axial line scan through the center of the circular defect after perpendicular lift-off of the magnet. B represents the radial residual magnetic leakage flux density.

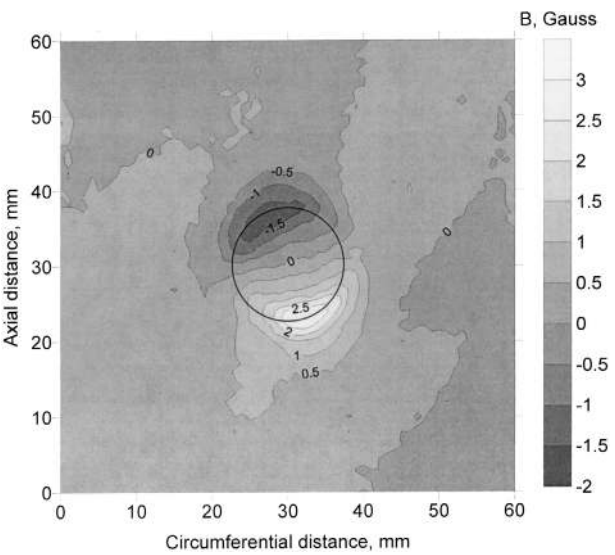

Fig. 6. Contour map of radial residual magnetic leakage flux density (B) after perpendicular lift-off of the magnet from the circular defect. Solid circle represents the actual location of the defect.

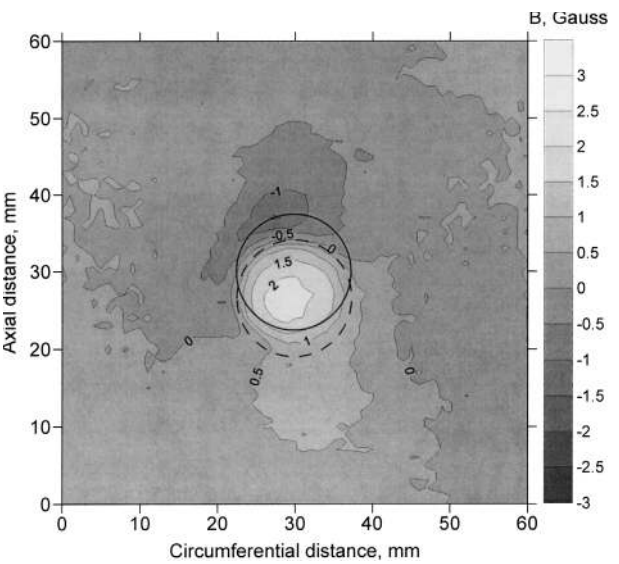

Fig. 8. Contour map of radial residual magnetic leakage flux density (B) after end lift-off of the magnet. Solid and dotted circles represent the actual and apparent locations of the defect, respectively.

The residual radial MFL scan and the corresponding axial line scan through the center of the defect are shown in Figures 6 and 7, respectively. These were obtained after lifting the magnet perpendicularly upward from the defect. The residual flux pattern shows magnetic polarity exactly opposite to that of active flux pattern of Figure 4. This is consistent with reports by Heath[7] for comparatively low excitation levels. The residual peak-to-peak flux density in the present case is about 4.3 G. It may also be noted from Figures 6 and 7 that, as for active flux patterns, the regions of positive and negative flux in the residual pattern appear to exhibit axial symmetry around the center of the defect. A small change in orientation of the flux pattern with respect to the axial direction is believed to be due to the rotation of the magnet after lifting it off the pipe. To summarize, as for active MFL patterns, the residual patterns with perpendicular lift-off can reveal information about the size and shape of the defect only on the basis of positions of high positive and negative flux regions. However, as with active MFL patterns, the shape of the defect is not directly obvious from the signal.

During actual service conditions the magnets always slide along the pipe axis; therefore subsequent residual scans were made after sliding the magnet along the axial direction on the outer surface of the pipe wall with south pole leading. The contour map and the line scan obtained with this end lift-off method are shown in Figures 8 and 9 and are markedly different from those shown for perpendicular lift-off. There is now a marked asymmetry between the regions of positive and negative

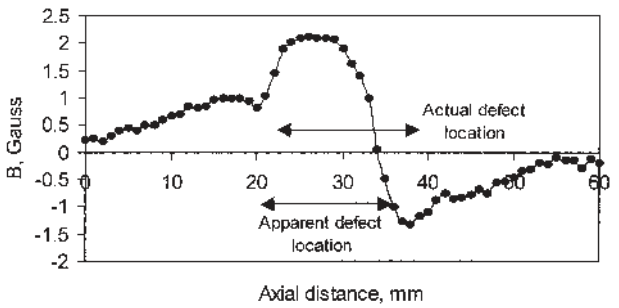

Fig. 9. Radial residual MFL axial line scan through the center of the circular defect after end lift-off of the magnet. B represents the radial residual magnetic leakage flux density.

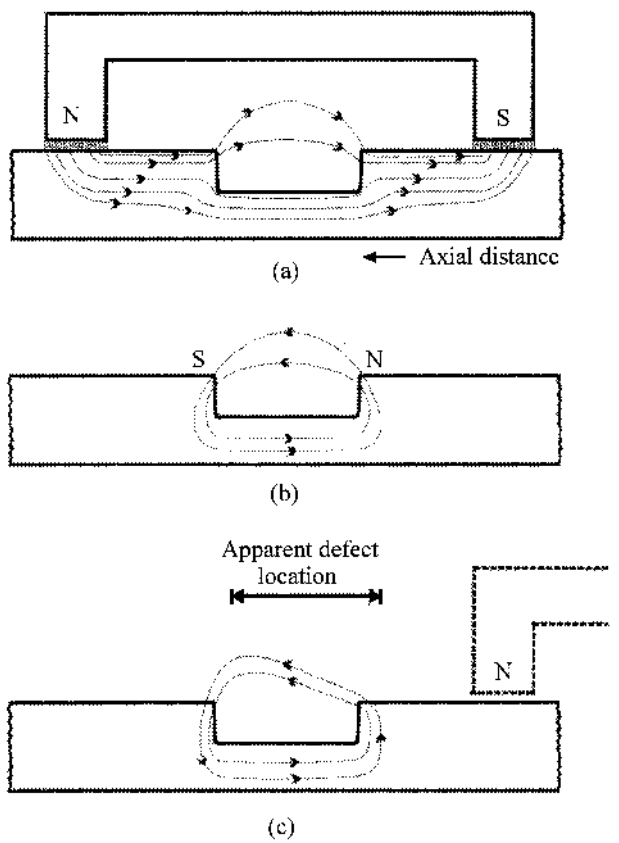

Fig. 10. Probable flux distributions around the circular defect: (a) active, (b) residual with perpendicular lift-off, and (c) residual with end lift-off.

flux; the center of positive and negative regions no longer coincide with the edges of the defect, and the region of positive flux is more spread out over the defect.

The possible active and residual flux distributions for the above cases are depicted in Figure 10. In the active case when magnet is on the defect, the flux and hence the domains are parallel to the top horizontal surface of the pipe, while those near the sides are oriented almost vertically. The path of flux lines near the edges of the defect is shown in Figure 10(a). When the magnet is lifted perpendicularly, the domains on either side of the defect tend to remain in the vertical orientation. A localized symmetric flux distribution is thus established around the defect, with flux being directed downward on the left, upward on the right, and from right to left over the defect. The flux path is shown in Figure 10(b) and is similar to that reported by Heath.[7] There appear to be induced south and north polarities near the edges of the defect along the axial direction. In the third case of end lift-off with north pole leaving the pipe at the end, the asymmetric flux distribution shown in Figure 10(c) appears to account for the asymmetric MFL pattern of Figure 9. This is due apparently to the slight displacement of the S-N dipole developed on the axial diameter of the defect toward the left, owing to the repulsion from the north pole of the magnet before end lift-off. However, there is a need to verify these results by other methods. Unfortunately, finite element model simulations cannot be used for this purpose unless the domain level phenomena are incorporated into the model.

One of the interesting features of the asymmetric contour map of residual MFL scan with end lift-off of the magnet is that the defect shape is reflected in the radial MFL signal. It is also easy to estimate the size and position of the defect. A close look at Figure 8 indicates an almost circular defect centered on a point of high positive flux marked by the dotted circle. The true location is marked by the solid circle and is slightly toward the negative flux region. The magnitude of the shift in the position of the defect apparently depends on the strength of the magnet and the magnetic properties of the pipeline and can be determined experimentally. It is about 3 mm for the present system. It is also possible to estimate the size of the defect from the axial line scan shown in Figure 9. The diameter of the apparent defect is approximately the length of the horizontal projection of the positive peak.

The active and residual radial MFL contour maps of the racetrack defect are shown in Figure 11. The solid racetrack boundary in Figure 11(a) indicates the true location of the defect, and the broken boundary in Figure 11(b) indicates its apparent location according to the residual signal. In the active scan, the ends of the defect are located slightly outside the positive and negative peak positions of the flux density but the shape and size of the defect cannot be seen clearly. Conversely, the residual scan gives a clear view of the size and shape of the defect, except with an axial shift of about 3 mm as observed in case of circular defect. The

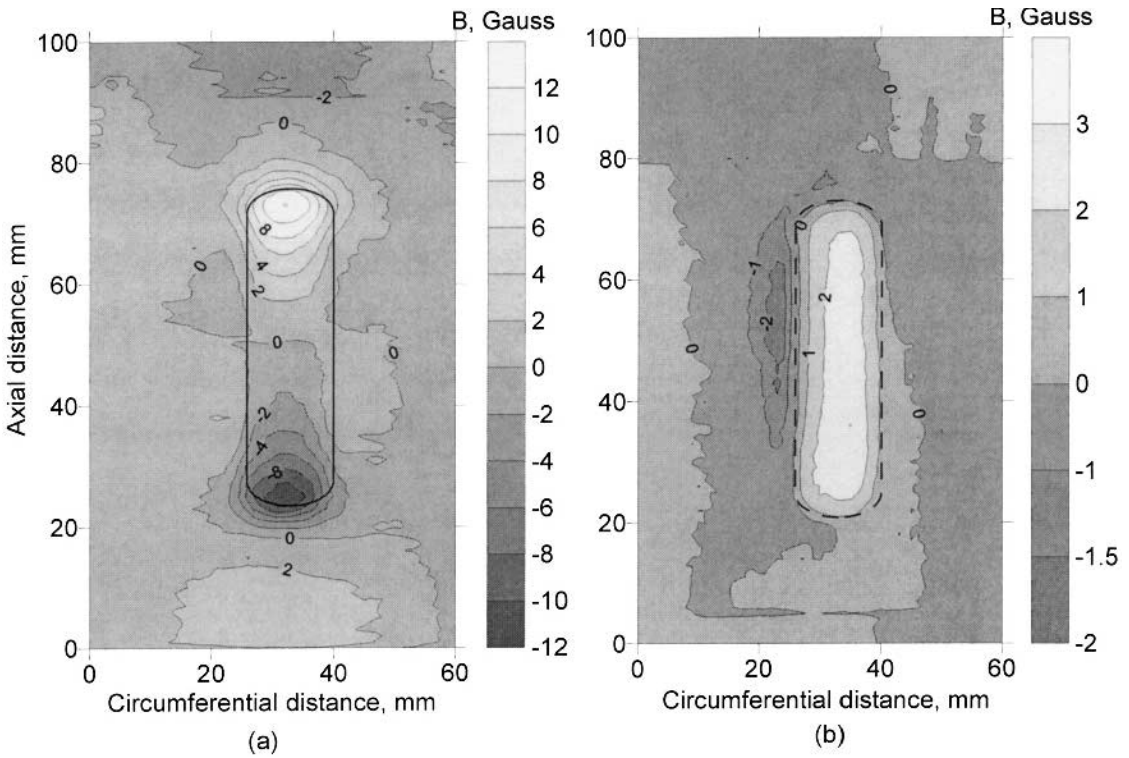

Fig. 11. Active (a) and residual (b) MFL radial contour maps of racetrack defect in the absence of stress. The actual and apparent locations of defect are indicated by the solid and broken racetrack boundaries, respectively.

nature of flux pattern of this residual scan, however, differs from that of circular defect. In the residual racetrack pattern, the region of high negative flux is not concentrated at the end of the defect, but on the axial side of it, while the region of high positive flux is present almost everywhere over the defect as observed for circular defect. This 90-degree rotation of the magnetic flux pattern from the expected axial direction is probably due to the large length of the defect, which does not permit the flux to make long axial loops. Instead, short circumferential flux loops around the defect are energetically more favorable wherein most of the flux lines emerge out of the defect, make loops around one of the long axial sides, and reenter the pipe slightly outside the region of defect. The domains are apparently aligned horizontally along the circumferential direction beneath the defect, but vertically along the axial wall of the defect. This is in spite of the fact that, even in the absence of applied stress, there exists a macroscopic easy axis that is parallel to the axis of the steel pipe section.[12,13]

The active and residual MFL scans of the third defect, an irregular gouge, are shown in Figure 12. Although the actual length, width, and maximum depression of the gouge are about 125 mm, 26 mm, and 14 mm, respectively, the overall depression is not limited to an area of just 125 mm $\times$ 26 mm because of depression of the surrounding region during the gouge formation. The defect is spread over a nonuniform area of about 155 mm $\times$ 65 mm as indicated in Figure 12 by the elongated closed contour. The active flux pattern of the gouge, as shown in Figure 12(a), does not exhibit longitudinal symmetry, which is expected owing to the nonuniformity in depression as well as width. The only resemblance this pattern has to the racetrack flux pattern of Figure 11(a) is that the upper half pattern shows a region of positive active flux and the lower half shows a region of relatively weak negative flux. The shape of the gouge is not apparent from this pattern. The extreme axial regions of high positive and negative flux are not due to the defect itself, but to the closer approach of the Hall probe detector to the magnetic brushes, where the induced magnetic poles produce spurious flux leakage signals. The residual flux pattern of Figure 12(b), on the other hand, shows a region of positive flux spread over the defect, which helps to estimate the size of the defect more conveniently. Thus, instead of active scans, the residual scans look

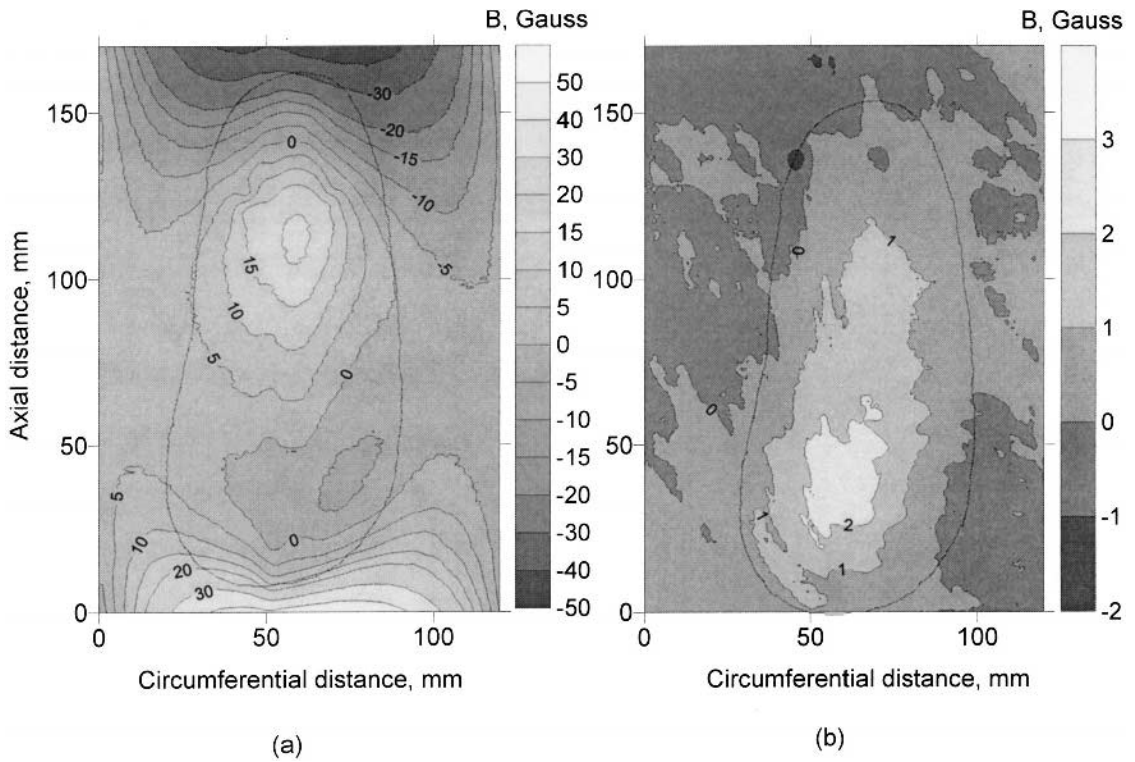

Fig. 12. Active (a) and residual (b) radial contour maps of the gouge in the absence of stress. The approximate location of the defect is shown in both.

more promising to reveal the size and shape of this type of irregular defect.

3.2 Active and Residual MFL Results as a Function of Pipe Wall Stress

In-service oil and gas pipelines are subjected to high stresses (up to 70% of the yield strength); thus the variations in the active MFL patterns brought about by the increased level of stress have been the subject of study.[14] When the pipe is axially magnetized, the higher circumferential stresses are known to affect the active MFL signals and patterns from circular blind-hole defects in two ways[15]: (1) they rotate the macroscopic magnetic easy axis of the pipe from the axial direction toward the circumferential direction, which causes the change in MFL_{pp}, and (2) they modify the MFL pattern by producing localized flux variations as a result of stress concentrations around defects. To study such changes in the residual MFL patterns, measurements were made on circular and racetrack defects at different stress levels. The main interest was to determine if, as at zero stress, the residual patterns could reveal the shape and size of the defects at high stress levels. Figure 13 depicts the residual MFL patterns of both circular and racetrack defects, which were magnetized at a stress level of 0 MPa but then studied at 220 MPa. The corresponding 0 MPa patterns are shown in Figure 8 and 11(b). A comparison of these patterns indicates that a flux rotation of 180 degrees occurs at stress values of 220 MPa, with positive and negative flux regions interchanging their locations. In the case of a circular defect, the negative flux region has two localized regions of comparatively higher flux along the circumferential or stress direction where the stress concentration is higher.[16] Two similar localized positive flux regions, though not clearly seen in Figure 13(a), are developed on the positive side of the flux at higher stresses. The positions of such localized flux regions may be linked to the localized stress concentrations around the defect. The residual pattern of the racetrack defect in Figure 13(b) also shows two pockets of positive and negative flux regions near the four corners of the racetrack.

The residual patterns of Figure 13 do not depict the shape of the defects as clearly as seen from patterns of Figures 8 and 11(b), which indicates that the application of stress reorients the magnetic domains along the stress direction, thus disturbing the original pattern.

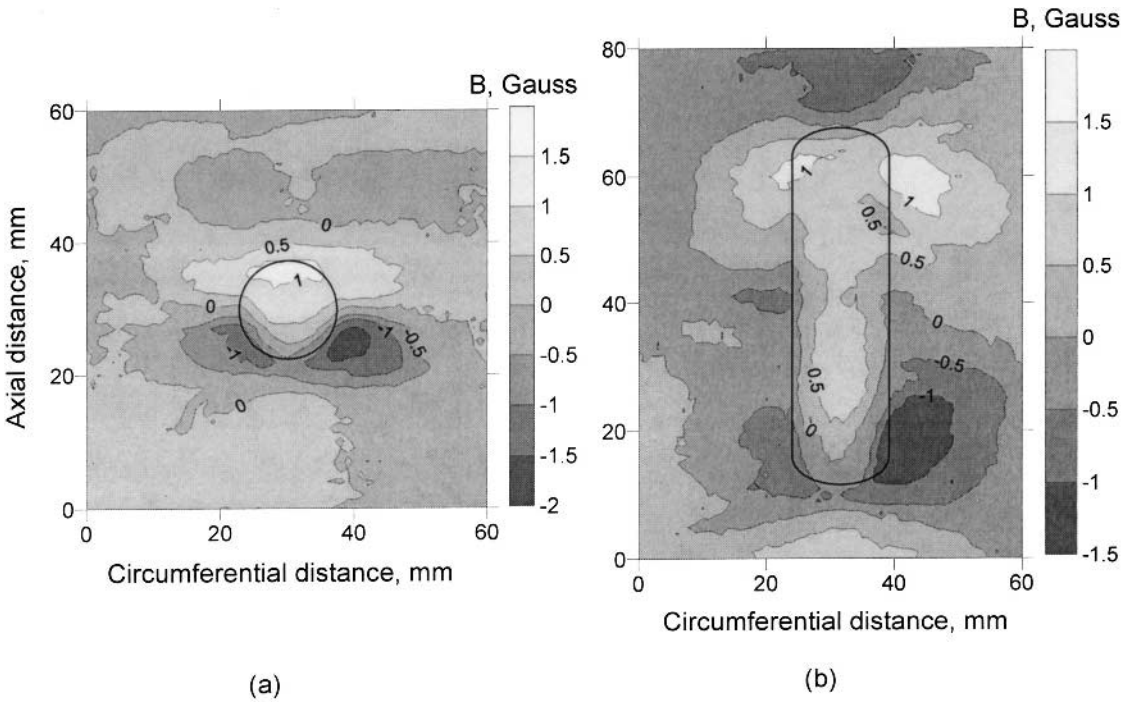

Fig. 13. Residual MFL scans of circular (a) and racetrack (b) defects taken at a stress of 220 MPa after magnetizing at 0 MPa. The actual defect locations are shown.

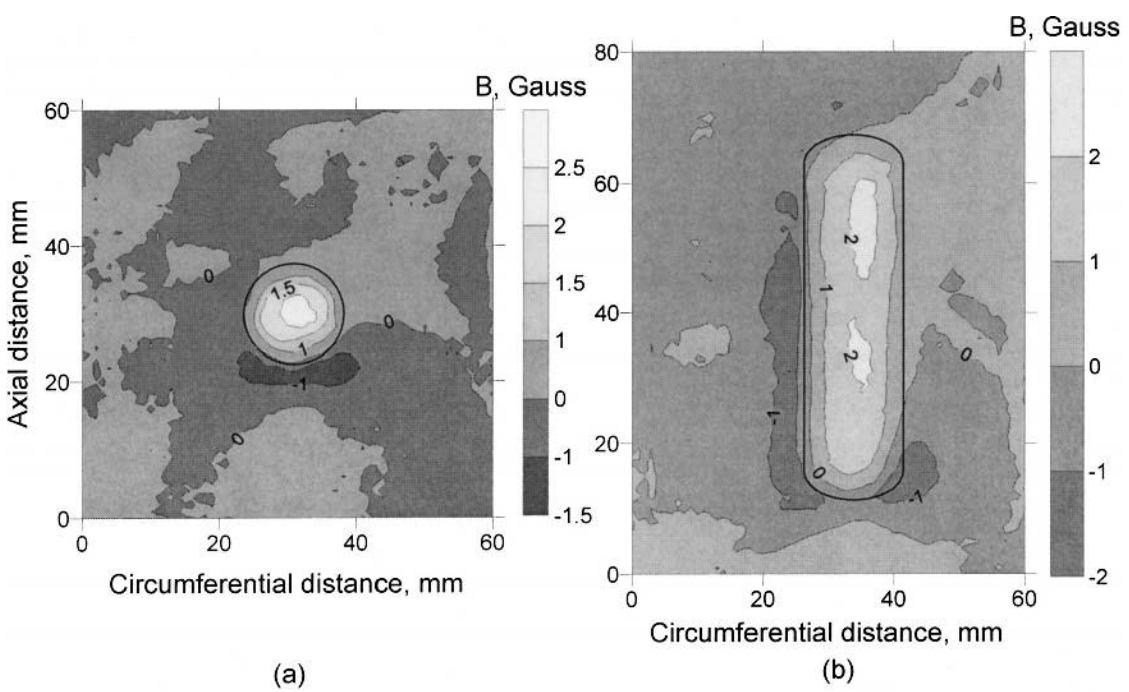

Fig. 14. Residual MFL scans of circular (a) and racetrack (b) defects taken at a stress of 220 MPa after magnetizing at the same stress. The actual defect locations are shown.

However, if the stress is applied before magnetization, as is done during inservice operation, the residual patterns can still be employed to get useful information about the shape and size of the defect. This is obvious from the residual patterns shown in Figure 14, where the defects were magnetized and also scanned at 220 MPa.

4. CONCLUSIONS

The residual MFL technique with end lift-off of the magnet appears to be very promising to provide useful information about defect geometry. Although the flux leakage signals weaken at high pressures, the technique still can be used to obtain reasonably good information provided the samples are magnetized at the same high pressure. However, the technique involves the use of sensitive probes to detect the flux leakage signals, which have about one tenth of the strength of the active flux leakage commonly used.

ACKNOWLEDGMENT

This research was supported by the Gas Research Institute, Natural Sciences and Engineering Research Council of Canada, and Pipetronix Ltd.

REFERENCES

1. D. L. Atherton, *Oil Gas J.* **87**, pp. 52–61 (1989).
2. R. E. Peterson, *Stress Concentration Factors*, (John Wiley & Sons, New York, 1974).
3. R. W. E. Shannon and L. Jackson, *Mater. Eval.* **46**, pp. 1516–1524 (1988).
4. D. L. Atherton, W. Czura, T. W. Krause, P. Laursen, B. Mergelas, and C. Hauge, *Proc. First Int. Pipeline Conf.* (Calgary, Canada, 1996).
5. K. Mandal, T. Cramer, and D. L. Atherton, The study of a race-track-shaped defect in ferromagnetic steel by magnetic Barkhausen noise and flux leakage measurements, *J. Magnetism Magnet. Mater* **212**, pp. 231–39 (2000).
6. D. L. Atherton and P. Laursen, *Proc. Pipeline Pigging Conf.* (Houston, TX, February 13–16, 1995).
7. S. E. Heath, Residual and Active Magnetostatic Leakage Field Modeling, MS Thesis (Colorado State University, Fort Collins, Colorado, USA 1984).
8. S. R. Satish, Finite Element Modeling of Residual Magnetic Phenomena, MS Thesis, (Colorado State University, Fort Collins, Colorado, 1980).
9. C. Hauge, Effects of line pressure on axially excited magnetic flux patterns, MSc Thesis (Queen's University at Kingston, Canada 1995).
10. R. Sabet-Sharghi, A neutron diffraction and magnetic Barkhausen noise evaluation of defect-induced stress concentrations, PhD Thesis (Queen's University at Kingston, Canada 1998).
11. C. R. Coughlin, L. Clapham, and D. L. Atherton, Effects of stress on MFL responses from elongated corrosion pits in pipeline steel, *NDT E Int.* **33**, pp. 181–188 (2000).
12. K. Mandal, D. Dufour, R. Sabet-Sharghi, B. Sijgers, D. Micke, T. W. Krause, L. Clapham, and D. L. Atherton, Detection of stress concentrations around a defect by magnetic Barkhausen noise measurements, *J. Appl. Phys.* **80**, pp. 6391–6395 (1996).
13. K. Mandal, D. Dufour, T. W. Krause, and D. L. Atherton, Investigations of magnetic flux leakage and magnetic Barkhausen noise signals from pipeline steel, *J. Phys. D: Appl. Phys.* **30**, pp. 962–973 (1997).
14. D. L. Atherton, T. W. Krause, and K. Mandal, Effects of stress on magnetic flux leakage and magnetic Barkhausen noise signals, *Rev. Prog. Quant. Nondestr. Eval.* **16**, pp. 1731–38 (1997).
15. T. W. Krause, R. W. Little, R. Barnes, R. M. Donaldson, B. Ma, and D. L. Atherton, Effect of stress concentration on magnetic flux leakage signals from blind-hole defects in stressed pipeline steel, *Res. Nondestr. Eval.* **8**, pp. 83–100 (1996).
16. P. Laursen, Effects of line pressure stress on magnetic flux leakage patterns, MSc Thesis (Queen's University at Kingston, Canada, 1991).